Appendix. Supplementary material

Impact of vaccination and non-pharmaceutical interventions on SARS-CoV-2 dynamics in Switzerland

Andrew J. Shattock[§1,2], Epke A. Le Rutte[§1,2], Robert P. Dünner[§1,2], Swapnoleena Sen[1,2], Sherrie L. Kelly[1,2,3], Nakul Chitnis[1,2], Melissa A. Penny[1,2*]

[1] Swiss Tropical and Public Health Institute, Basel, Switzerland
[2] University of Basel, Basel, Switzerland
[3] Burnet Institute, Melbourne, Australia
[§] Contributed equally
*Corresponding author (melissa.penny@unibas.ch)

This supplementary material provides additional details, including equations and visualisations, for the OpenCOVID model and an application to the COVID-19 epidemic in Switzerland. This document accompanies the manuscript "Impact of vaccination and non-pharmaceutical interventions on SARS-CoV-2 dynamics in Switzerland".

Model calibration

OpenCOVID was calibrated to the national-level epidemic in Switzerland using publicly available epidemiological data from the Swiss Federal Office of Public Health (1). Model output was matched to six types of observed temporal metrics: 1) daily confirmed COVID-19 cases, 2) daily COVID-19-related deaths, 3) daily hospital admissions, 4) number of COVID-19 patients in hospital, 5) number of COVID-19 patients in ICU, and 6) relative prevalence of virus variants (2). Figure S.1 shows the alignment of the model output to the epidemiological data, along with several additional model metrics. Age-disaggregated metrics are illustrated in Figure S.2. The alignment of the model to data got the prevalence of viral variants is shown in Figure S.3. See Table S.1 for a full list of calibrated and fixed model parameters.

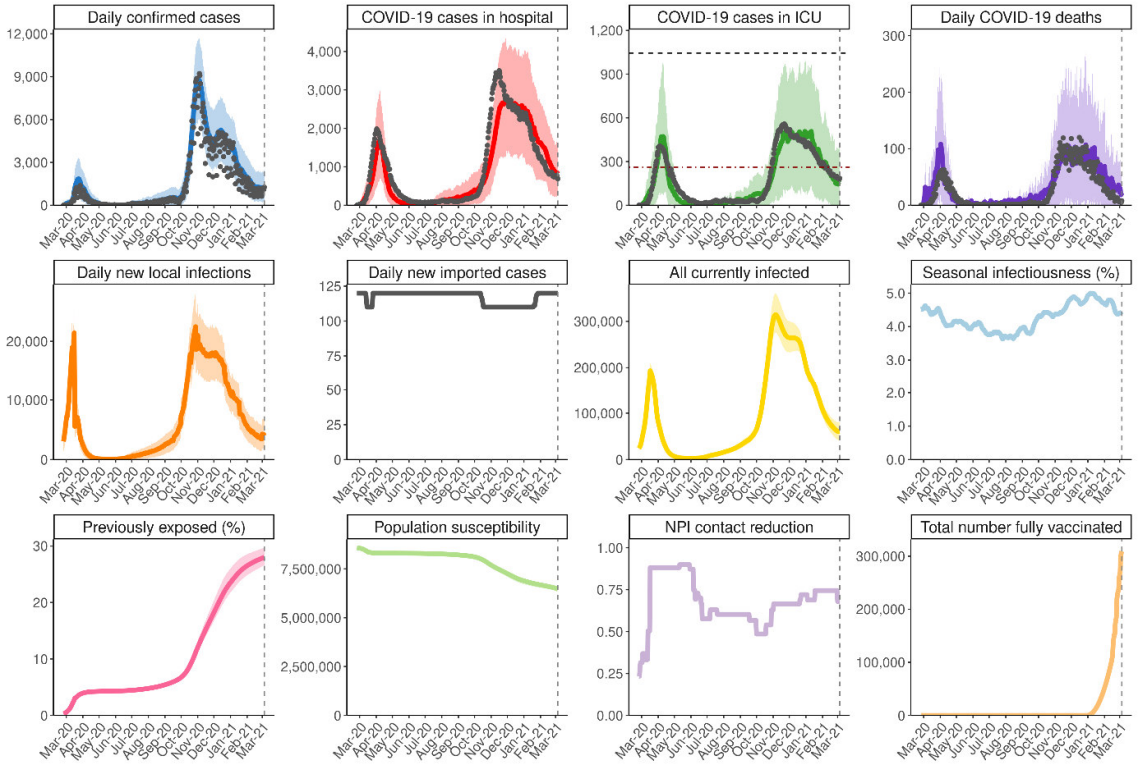

Figure S.1: OpenCOVID calibrated to national-level data of confirmed cases, hospitalisations, ICU occupancy, and deaths in Switzerland up to 5 March 2021. Black dots represent the data to which the model has been calibrated. Coloured lines represent model output.

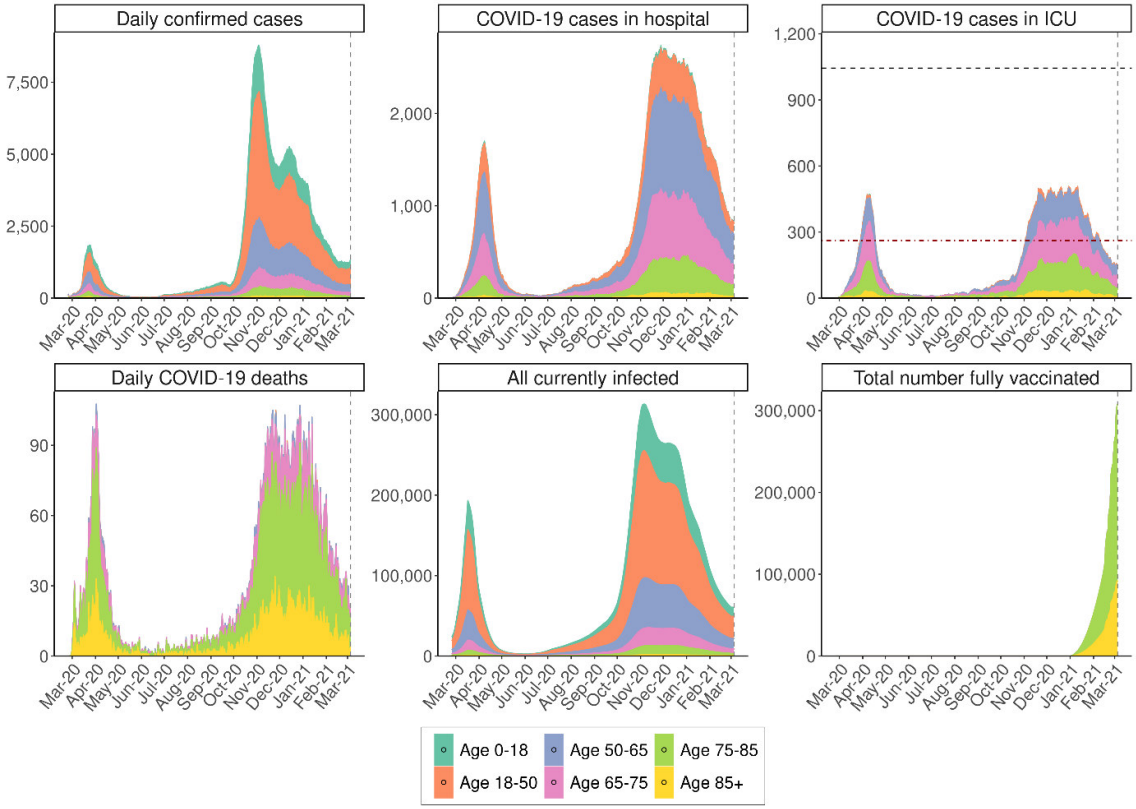

Figure S.2: Daily confirmed cases, COVID-19 cases in hospital, COVID-19 cases in ICU, daily COVID-19 deaths, all currently infected, and total number fully vaccinated by age group. Outputs are shown for the calibrated period between 18 February 2020 and 5 March 2021.

Table S.1: Calibrated and fixed model parameters with sources

Model parameter	Description	Calibrated value or fixed distribution	Truncation bounds	Specifications and sources
contacts	Number of contacts per person per day, where a contact has a transmission probability of beta	11.4	5 – 25	Calibrated See *Contact network* section
beta	Baseline probability of transmission in one contact between a fully susceptible individual (i.e., no partial or sterile immunity) and a fully infectious individual (i.e., when viral load is at maximum)	$X = 0.05$	Not applicable	Not calibrated See *Infectiousness per contact* section
seasonality_scaler	Multiplicative factor for effect of temperature on transmission probability per contact	0.27	0.2 – 0.8	Calibrated See *Seasonality* section
proportion_asymptomatic	Proportion of all cases that are asymptomatic	$X \sim N(0.3, 0.02^2)$	0.2 – 0.4	Not calibrated (3-8)

Model parameter	Description	Calibrated value or fixed distribution	Truncation bounds	Specifications and sources
presymptomatic_days	Number of days infectious before showing symptoms	$X \sim N(3, 0.5^2)$	1 – 5	Not calibrated (9-13)
latency_days	Number of days in latency (infected but not infectious) state	$X \sim N(4.6, 1^2)$	3 – 7	Not calibrated (9-13)
infectious_days_mild	Number of days for which non-severe cases are infectious (excluding presymptomatic phase)	$X \sim N(6, 1^2)$	3 – 10	Not calibrated (9, 14-16)
infectious_days_severe	Number of days for which severe cases are infectious (excluding presymptomatic phase)	$X \sim N(28, 1^2)$	14 – 30	Not calibrated (13, 17-20)
seek_hospital	Proportion of severe cases that will seek hospital care	0.41	0.4 – 0.95	Calibrated Assumed prior distribution (1)
onset_to_hospital_days	Number of days between symptom onset and hospitalisation	13.4	1 – 14	Calibrated (1, 13, 17, 21-23)
diagnosis_delay	Delay between symptom onset and test (and diagnosis)	$X \sim N(3, 0.5^2)$	0 – 5	Not calibrated (24)
reporting_delay	General reporting delay for all epidemiological and hospital metrics	$X \sim N(1, 0.1^2)$	0 – 4	Not calibrated Assumed
isolation_probability	Proportion of mild and asymptomatic cases that isolate after diagnosis	$X = 1$	Not applicable	Not calibrated Assumed
isolation_duration	Number of days spent in isolation after diagnosis	$X = 10$	Not applicable	Not calibrated (16)
hospital_stay_days	Number of days a severe non-critical case spends in hospital before discharge	$X \sim N(9, 1^2)$	7 – 20	Not calibrated (13, 17, 21, 23, 25)
hospital_to_icu_days	Number of days between hospital admission and ICU admission for cases that will become critical	$X \sim N(2, 1^2)$	1 – 10	Not calibrated (23, 26)
icu_stay_days	Number of days a critical case spends in ICU before transfer back to non-ICU ward	$X \sim N(7, 1^2)$	1 – 14	Not calibrated (13, 17, 21, 23, 25)
icu_stay_death_days	Number of days a critical case spends in ICU before death	$X \sim N(6, 1^2)$	3 – 14	Not calibrated (13, 17, 20, 23, 25)
hospital_transfer_days	Number of days spent in non-ICU ward following discharge/transfer from ICU	$X \sim N(2, 0.1^2)$	1 – 7	Not calibrated (22)
home_death_days	Number of days between symptom onset and death for those not seeking hospital care	$X \sim N(10, 1^2)$	7 – 14	Not calibrated Assumed
death_reporting_delay	Additional delay between a COVID-19 death and that death being reported in the data	$X \sim N(2, 0.2^2)$	1 – 14	Not calibrated (21, 22)

Model parameter	Description	Calibrated value or fixed distribution	Truncation bounds	Specifications and sources
critical_death_icu	Proportion of critical cases that die in ICU care (ventilators assumed to be available)	0.63	0.4 – 0.8	Calibrated (1, 21, 22)
critical_death_non_icu	Proportion of critical cases that die when ICU not available or not sought	$X \sim N(0.95, 0.1^2)$	0.5 – 0.99	Not calibrated (21)
improved_care_factor	Proportionate reduction in probability of severe cases becoming critical cases (and requiring ICU) due to improved care and treatment procedures	0.72	0.40 – 0.99	Calibrated (27)
import_date	Number of days delay between first case importation and first confirmed case	$X = 7$	Not applicable	Not calibrated Correlated with import_initial
import_initial	Number of people (per 100,000) initiated with infection import_date number of days before first confirmed cases	78	1 – 100	Calibrated Assumed prior distribution
import_constant	Number of imported cases per 100,000 people per day	1.4	0.1 – 5	Calibrated Assumed prior distribution
npi_scaler	Calibration factor for proportionally scaling the Oxford Health and Containment Index (OCHI) to derive a reduction in effective contacts	1.3	0.8 – 1.5	Calibrated See *Non-pharmaceutical interventions* section
acquired_immunity	Initial level of acquired immunity due to infection	$X \sim N(0.83, 0.1^2)$	0.76 – 0.87	Not calibrated (28, 29)
vaccine_immunity_days	Number of days following vaccination (first dose) until full efficacy is attained	$X = 28$	No bounds assumed	Not calibrated (30)

Variants of concern

OpenCOVID tracks transmission chains of viral variants. The model can consider any number of variants, providing there is sufficient data to inform the relative prevalence of each variant in the population. Three viral variants were modelled in this application of Switzerland: D614G (considered the dominant variant at the start of the epidemic (31)), B.1.1.7 (2, 32), and B.1.351 (S501Y V2) (33). Figure S.3 shows the alignment of the calibrated model to variant prevalence over time. We modelled the B.1.1.7 and B.1.351 variants by assigning them a percentage increase in the probability of transmission per contact (34, 35), then further calculated the likely transmission advantage in a heterogeneous population with pre-existing immunity during an ongoing pandemic with existing non-pharmaceutical interventions (captured in our individual-based model). We estimated the effective reproductive number, R_e, of B.1.1.7 for the months of January and February, for the specified increase in the transmission probability, assuming a serial interval of 6-days and calculated the transmission advantage as the ratio of the effective

reproductive number to that of variant D614G. We further conducted a sensitivity analysis varying the serial interval (3-9 days).

The transmission advantage is therefore the proportional increase in the expected number of cases from one infected individual in the epidemic setting in Switzerland in early 2021 (including the effects of pre-existing natural immunity and the impact of control measures). It is thus important to note that a 60% increase in the probability of transmission per contact does not correspond to a 60% increase in the effective reproductive number, R_e, but rather closer to a 30% increase. Allowing for variation in the serial interval, this can vary between 10% and 50%. The scenario with a 70% increase in transmissibility corresponded to a transmission advantage of 1.4 (1.2-1.6); and that with a 50% increase in transmissibility corresponded to a transmission advantage of 1.2 (1.1-1.4).

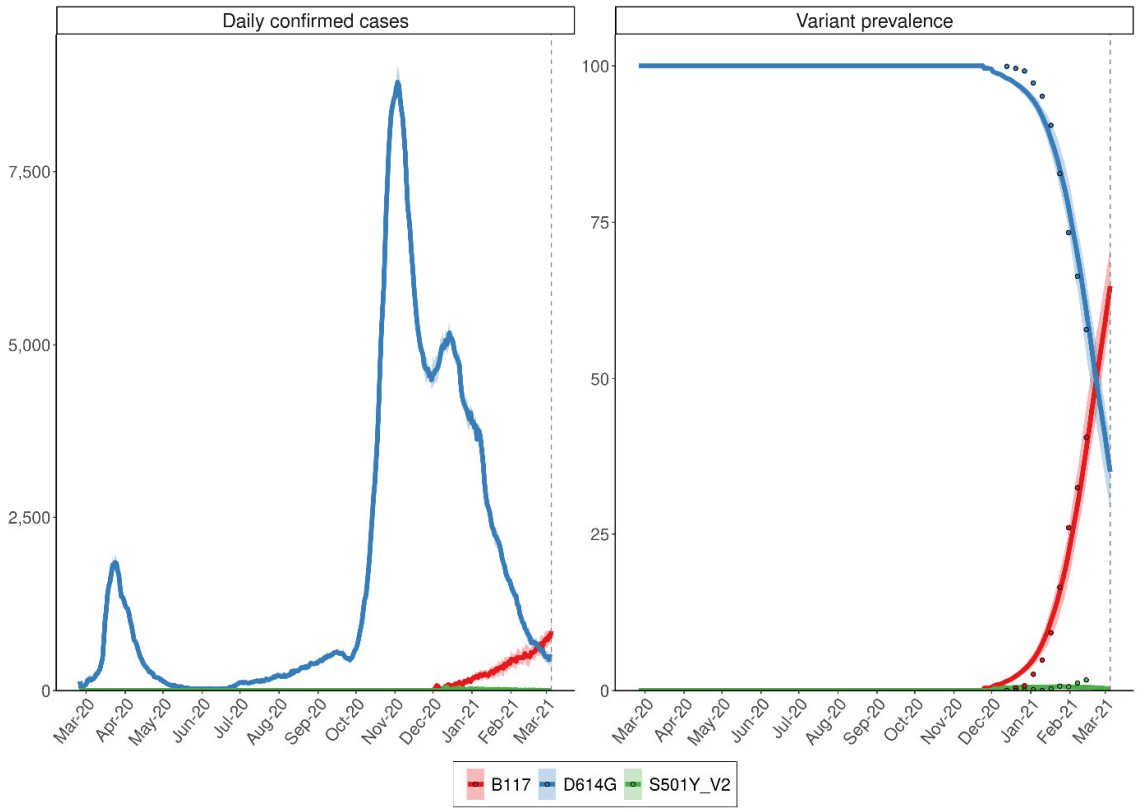

Figure S.3: Calibrated variant dynamics in Switzerland until 5 March 2021. Blue is the D614G variant which was dominant in Switzerland from summer 2020 on and is used here synonymously with the earlier strains circulating in Switzerland due to their epidemiological similarity. Red is the B.1.1.7 variant with a 60% increased infectivity. Green is S501Y V2 (B.1.351) with a 10% increased infectivity. The solid lines are the model fit; the coloured points represent data.

Table S.2: Baseline properties of viral variants modelled for this application of Switzerland

Viral variant	Model import date	Number imported (per 100,000 people)	Infectivity factor	Disease severity factor
D614G	See Table S.1	Calibrated (See Table S.1)	1 Reference variant (31)	1 Reference variant (31, 36)
B.1.1.7	24 November 2020	12	1.6* [1.5-1.7]	1* [1-1.5]
B.1.351	1 December 2020	8	1.1	1

* Sensitivity of model outputs to varying infectivity and disease severity factors were quantified within the sensitivity analysis.

Likelihood and calibration details

The calibration process for this application to Switzerland was as follows: 4,000 parameter sets were initially sampled across parameter hyperspace. That is, the region defined by the bounds of each calibrated parameter in Table S.1 (calibrated parameters highlighted in blue). A Latin hypercube algorithm was used for this initial sampling; thus, no focus was placed on regions in which parameter priors are located. Each parameter set was then simulated 10 times for different stochastic realisations using OpenCOVID, thus capturing a basic understanding of stochastic uncertainty. All model simulations were performed simultaneously on a high-performance computing cluster (37). The value of a log-likelihood objective function was calculated for each parameter set, quantifying the likelihood of model parameters given the epidemiological data illustrated in and Figure S.1 and Figure S.3. The log-likelihood function is given by:

$$L = \sum_i \bar{l}_i(\bar{m}_i, \bar{d}_i) \cdot \omega_i$$

$$\bar{l}_i(\bar{m}_i, \bar{d}_i) = ln\left(\left[\frac{1}{(\bar{d}_i - 1)!}\bar{m}_i{}^{\bar{d}_i - 1} e^{-\bar{m}_i}\right] \cdot \bar{\tau}\right)$$

Where:

- $\bar{m}_i = ({m_i}^1, {m_i}^2, \dots, {m_i}^n)$ represents model output for metric i, and
- $\bar{d}_i = \left({d_i}^1, {d_i}^2, \dots, {d_i}^n\right)$ represents the observed epidemiological data for metric i.

The values ${m_i}^1$ and ${d_i}^1$ represent the first date for which we have non-zero data for metric i, starting from 24 February 2020, whilst ${m_i}^n$ and ${d_i}^n$ represent the final date for which we use data in the model calibration process. In this application of Switzerland, n represents 5 March 2021. The vector $\bar{\tau} = (\tau^1, \tau^2, \dots, \tau^n)$ is the time weight vector, where $\tau^j \in [0, 1]$ for all j. In this application $\bar{\tau}$ is defined to linearly increase from 0.5 to 1 between 24 February 2020 and 5 March 2021. The constant ω_i is the weighting applied to metric i. These weightings used for this application are shown in Table S.3.

Table S.3: Weightings of calibration metrics in likelihood function

Metric	Weighting (ω_t)	Comments
Daily confirmed cases	1	Default weighting
Daily COVID-19 deaths	2	Higher weighting to account for higher reporting probability
New daily admissions to hospital	0	No weighting applied due to discrepancies between data sources
COVID-19 cases in hospital	4	Higher weighting to account for higher confidence in reporting
COVID-19 cases in ICU	4	Higher weighting to account for higher confidence in reporting
Variant prevalence	1.6	Weighting of 50 applied to 12 data points implies a relative weighting of 1.6

A Gaussian Process model was then trained using all parameter sets and associated likelihood values to predict the log-likelihood over all data given a model parameter set. For this analysis, we used a heteroscedastic Gaussian Process algorithm as the model emulator (38, 39). Ten rounds of adaptive sampling were applied to efficiently resample regions of the parameter hyperspace that were good candidates for the global maximum. An expected improvement acquisition function was used to identify these candidate regions and sample 100 new parameters sets per round, with a filtering function applied to ensure resampled parameters sets are not within a predefined distance of each other (with distance measured in Manhattan space). Following the ten rounds of adaptive resampling, the simulated parameter set with the highest log-likelihood value (considering the mean over all stochastic simulations) was identified as the best estimate parameter set, as reported in Table S.1. See Figure S.1 and Figure S.3 for alignment of model outcomes to the observed data.

Infectiousness per contact

In OpenCOVID, we define a pairwise transmissible contact to be a human-to-human contact that has a transmission probability of β when the infectious individual is fully infectious, and the susceptible individual is fully susceptible. An individual is fully infectious when their viral load is at a maximum (see *Viral load profile* section). An individual is considered to be fully susceptible when they have zero immunity (see *Immunity* section). We note here that in this application, both previously infected and vaccinated individuals will possess a non-zero level of immunity. Two additional factors can alter the probability of transmission between and infectious individual and a susceptible individual. First, a seasonality effect reduces the probability of transmission in warmer periods, reflecting a larger proportion of contacts being outdoors with warmer temperatures (see Seasonality section). Second, novel viral variants can enter the population, being more (or less) infectious than the current dominant variant, and therefore increase (or decrease) the probability of transmission. For this study, we assume the SARS-CoV-2 epidemic in Switzerland began with variant D614G being the dominant variant Figure S.3. For this study, we defined β to be 5% (see Table S.1). That is, we define a contact to have a 5% probability of transmission when the infectious person has a peak in viral load, the susceptible person has no partial immunity, the contact is during the coldest day of the year, and the variant being transmitted in D614G. With the value of β fixed, the population average number of contacts can then be calibrated such that observed epidemiological data is matched (see sections *Contact network*, *Model calibration*, and Table S.1).

In equation form, the probability of transmission between an infection individual, I, and a susceptible individual, S, is given by:

$$P(\text{transmission}) = \beta \cdot v_I(\tau) \cdot \varphi_I \cdot \sigma(t) \cdot \ (1 - \mu_S)$$

Where:

- $v_I(\tau) \in [0, 1]$ denotes the viral load of the infectious individual, τ days following infection (see *Viral load profile* section).
- φ_I denotes the infectivity factor of the viral variant with which the infectious individual is infected (see Table S.2 in *Variants of concern* section).
- $\sigma(t)$ denotes the seasonality scaler at date t (see *Seasonality* section).
- μ_S denotes the immunity of the susceptible individual (see *Immunity* and *Vaccine properties* sections).

Contact network

The contact network in OpenCOVID is based on the POLYMOD contact survey (40) which reports age-structured contact frequencies. The POLYMOD survey is implemented in OpenCOVID via the R package socialmixr (41) which provides symmetric matrices in which the rows and columns are the age class of the ego (the person reporting the contact) and the alter (the person receiving the contact), and the cell content is the average number of contacts between those age classes. This data can be accessed by country. As POLYMOD does not provide Swiss survey data, we use artificial contact frequencies based on survey data from France, Germany, and Italy. We then use Swiss age-structured demographic data to sample this contact frequency space and create an age-structured random network by sampling with replacement, weighted by the average number of contacts per cell. We sample such that the resulting network has a mean number of contacts (as defined by the 'contacts' parameters, see Table S.1). In such a network, not all age classes have the same number of contacts. Younger age classes have more contacts and especially have more contacts with other young age classes while older age classes have fewer contacts Figure S.4. This captures the qualitative aspect of an age structured network based on European survey data, and then transforms to Swiss specific demography. This network does not distinguish between work, school or home networks but is rather integrated across all these separate networks. Individual ages are tracked for 0-90 years in one-year age bins, with an additional group for 90+. Gender is not considered in the model (42).

With β (the infectiousness per contact, see *Infectiousness per contact* section) set at a fixed value (see Table S.1), the population average number of contacts can then be calibrated such that observed epidemiological data is matched. The primary signal for the contacts parameter is the exponential increase in all observed metrics during the first wave prior to the observed impact of NPIs.

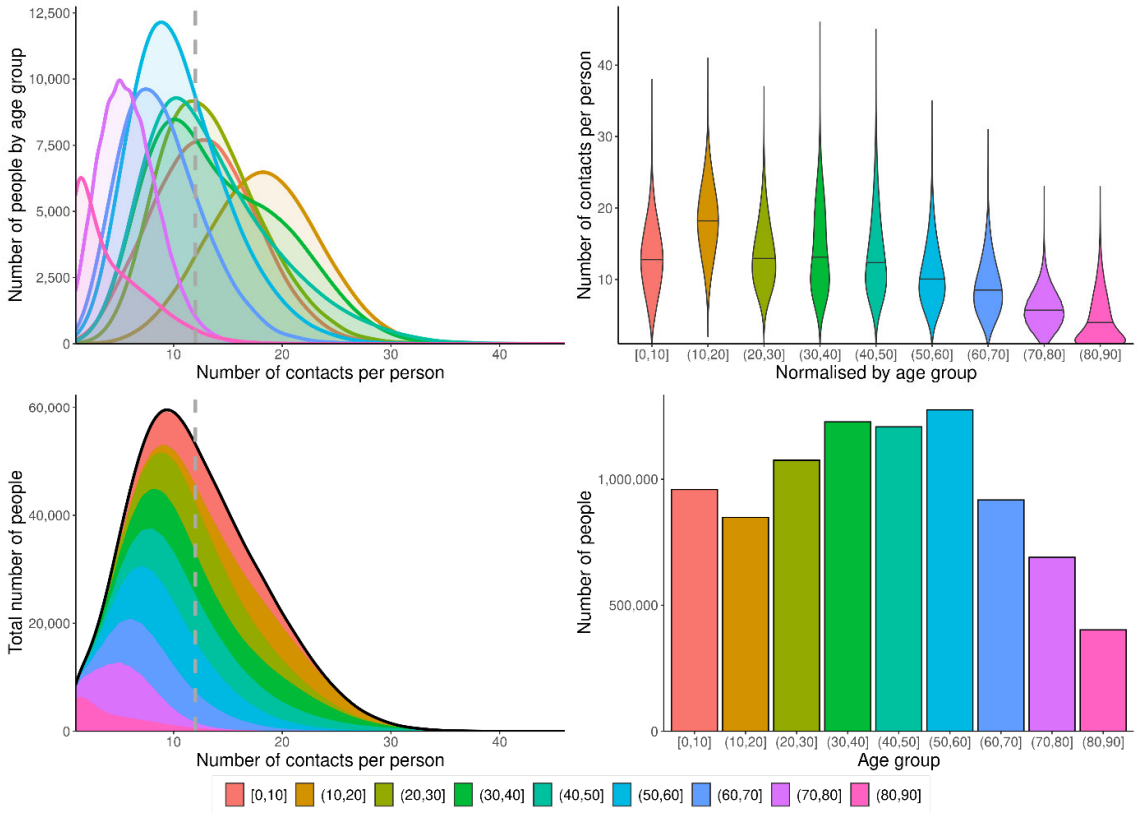

Figure S.4: Age-related contact properties in OpenCOVID for this application to Switzerland. Top: Number of people in age group vs. number of contacts per person. Shows both the groups' sizes and the distribution of contacts. Note that younger people have more contacts. Top right: Normalized number of contacts per person vs. age group. Again, shows the distribution of the average number of contacts per person in an age group. The age group of 10 to 20 year olds has the highest number of contacts. Bottom left: Total number of people vs. number of contacts per person. Bottom right: Number of people vs. age group. Shows the distribution of age group sizes.

Viral load profile

During the latent period that follows infection, we assume viral load is zero (and therefore that the infected person is not yet infectious). We then use a gamma probability density function with shape parameter $\alpha = 3$ and rate parameter $\beta = 0.5$ to represent individual-level viral load over the course of the infectious period. We assume infectiousness is proportional to this viral load (43), and therefore standardise viral load values to between zero and one to convert viral load into an infectiousness scaler that scales the probability that the individual can infect other contacts. The parameters of the gamma function were selected to best represent the current understanding of viral load profiles from time since infection (9, 44). Figure S.5 illustrates this infectiousness scaler (multiplier) profile from the time since infection.

In equation form, the infectiousness scaler for an individual k infected τ days after infection is given by:

$$v(\tau) = \begin{cases} 0, \tau < l \\ v'(\tau), x \geq l \end{cases}$$

Where l is the sampled latent period for individual k (see *Infection, disease, and hospitalisation durations* for duration distributions) and

$$v'(\tau) = \frac{\beta^{\alpha}(\tau - l)^{\alpha-1}e^{-\beta(\tau-l)}}{(\alpha - 1)!}$$

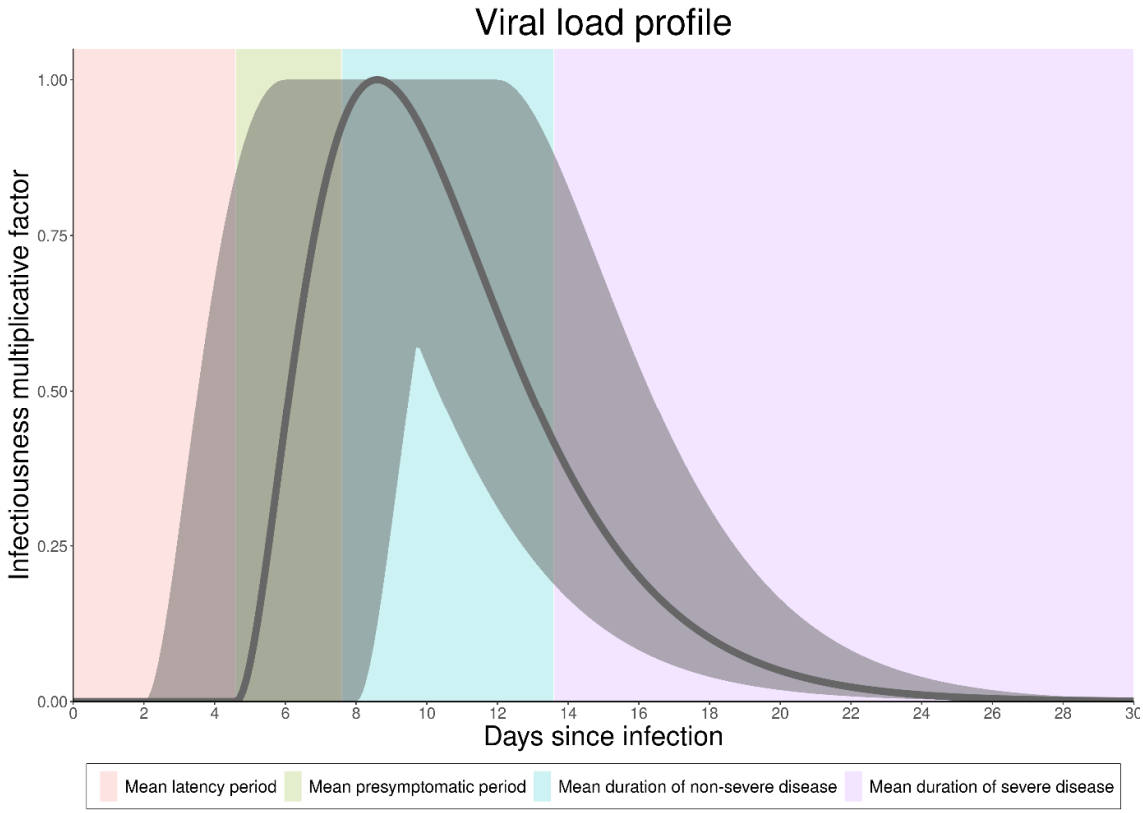

Figure S.5: Viral load profile from time since infection. Curve is standardised to between zero and one to yield an infectiousness multiplier used to calculate the probability of transmission. Peak infectivity is reached between day 6 and day-14 following infection.

Seasonality

We take daily temperature data from the federal office of meteorology and climatology MeteoSwiss (45), which is made available via the opendata.swiss service (46). We use the daily maximum temperature values that are available from the NBCN measurement station network (47). These stations provide different daily weather data across Switzerland. Nevertheless, not

all cantons have stations, and some cantons have several stations. For national level analyses we use averaged data across all available weather stations. For cantons with multiple weather stations, we take the mean value across all stations. We then use a population-weighted mean to derive national level values. In Figure S.6, the grey lines represent temperature data from 1 January and 5 March 2021 (date of calibration). Over this time period, the yellow line represents the population-weighted national average. From 6th March onwards, the line represents the future projection of temperature. This future projection uses monthly data from years 1981-2010, and is generated by a spline fitting algorithm form the R package RMAWGEN (48). The seasonality effect used in the model (see *Infectiousness per contact* section) is then derived from the normalized inverse of the temperature curve.

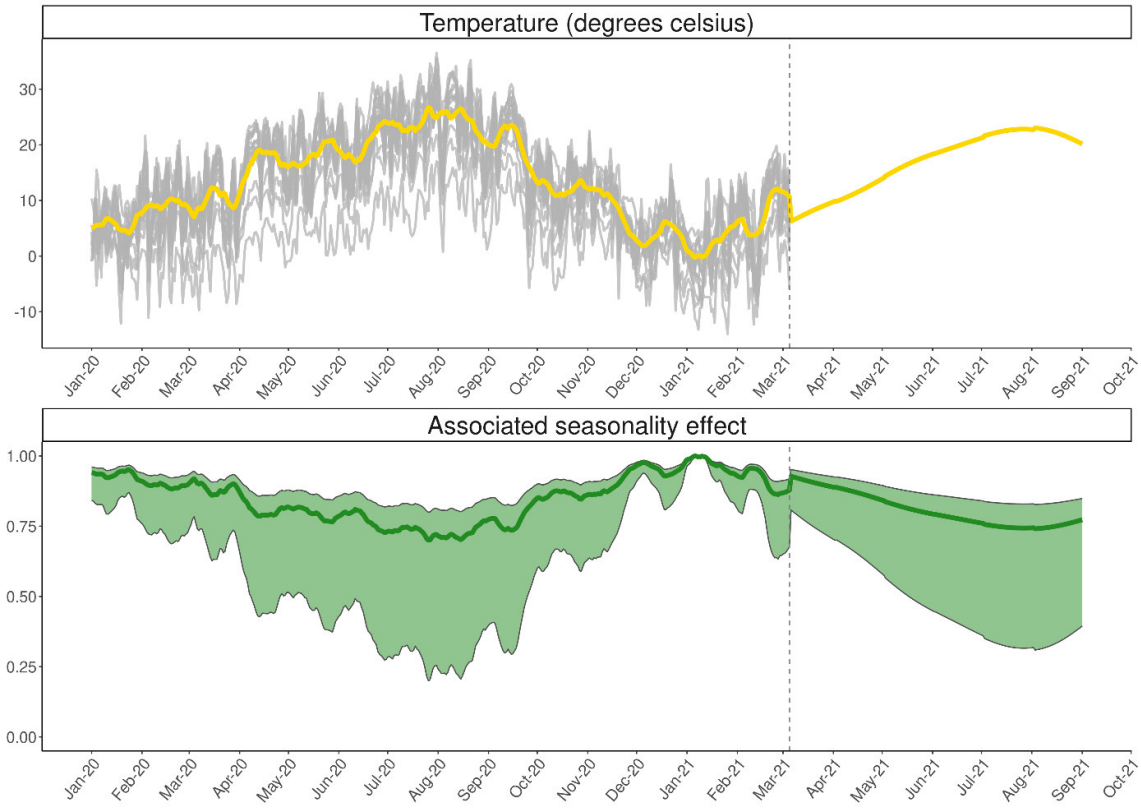

Figure S.6: Temperature and associated seasonality effect in OpenCOVID. Grey lines represent past cantonal temperatures, and the yellow line represents the population-weighted national average. The green line represents the associated best estimate seasonality effect. That is, with a seasonality scaler of 0.27 (as reported in Table S.1). The green shading represents the range of possible seasonality effects, considering the bounds of the seasonality scaler.

Non-pharmaceutical interventions

In OpenCOVID non-pharmaceutical interventions (NPIs) can curb the spread of SARS-CoV-2 by reducing the number of potentially transmissible pairwise contacts. In Switzerland, such measures have included the closing of non-essential shops, restrictions on mass gatherings, and facemask mandates in publicly accessible spaces. The Oxford Containment and Health Index (OCHI) is a measure that is proportional to the amount (or stringency) of such measures that are in place at a moment in time (14). The OCHI ranges from 0 to 100, with 0 being no measures in place and 100 being the most restrictive full lockdown possible. The level of the OCHI, together with a calibrated multiplicative scaling parameter is used in OpenCOVID to capture the effect of NPI in reducing the effective daily number of contacts. In effect, the edge list associated with the contact network – that is, the list of all daily pairwise contacts in the network – is reduced by a proportion given by the product of the OCHI on a given day and the calibrated NPI scaling constant (see Table S.1). In this manner, we do not explicitly simulate the effect of individual measures, but instead model the total effect of all NPIs in place.

The Swiss level of the OCHI is collected at the cantonal- and federal-level based on publicly-available information from various sources, and is available from the Swiss TPH GitHub (49). This publicly available information is translated into 16 Swiss specific variables, and from there into the 12 variables that together make up the Oxford Containment and Health Index. The Swiss TPH GitHub on the Swiss measures provides a codebook for the Swiss specific variables. For an overview of the variables that make up the Oxford Containment and Health Index, their coding schemes and how to calculate the OCHI from the constituent variables, the reader is referred to the codebook, the coding interpretation guide, and the instruction on how to calculate indexes provided by the Blavatnik School of Government at the University of Oxford (14).

Figure S.7 shows the value of the Oxford Containment and Health index, that is representative of the strength of measures as applied in Switzerland, for past data (left of the vertical black dashed line) as well as an example scenario of future NPI relaxation (right of the vertical black dashed line) which corresponds to the red scenario from manuscript Figure 2. This scenario considers three different five point NPI relaxation steps, from 58.5 to 53.5 on 22 March 2021, to 48.5 on 12 April, and to 43.5 on 5 May. The five percentage point relaxation steps were chosen to approximately represent a potential NPI relaxation package published by the Federal Council on 17 February 2021 (50). This potential package included increasing the limit on indoor private events from 5 to 10, opening professional sporting and cultural events at one-third capacity, and reopening restaurants for outside service. It is important to note that not all openings have a quantitative effect on the OCHI. We stress here that the specific openings are not modelled explicitly, but rather the abstraction of an equivalent amount of NPI relaxation that is reflected in the OCHI. Moreover, the same amount of opening in terms of OCHI can also be reached with different combinations of openings, so that the OCHI stays agnostic to a specific type of opening, and only reflects a certain amount of opening. We provide all gathered detailed information on the measures that were in place at all dates, both at the cantonal and national level on the Swiss TPH GitHub (49).

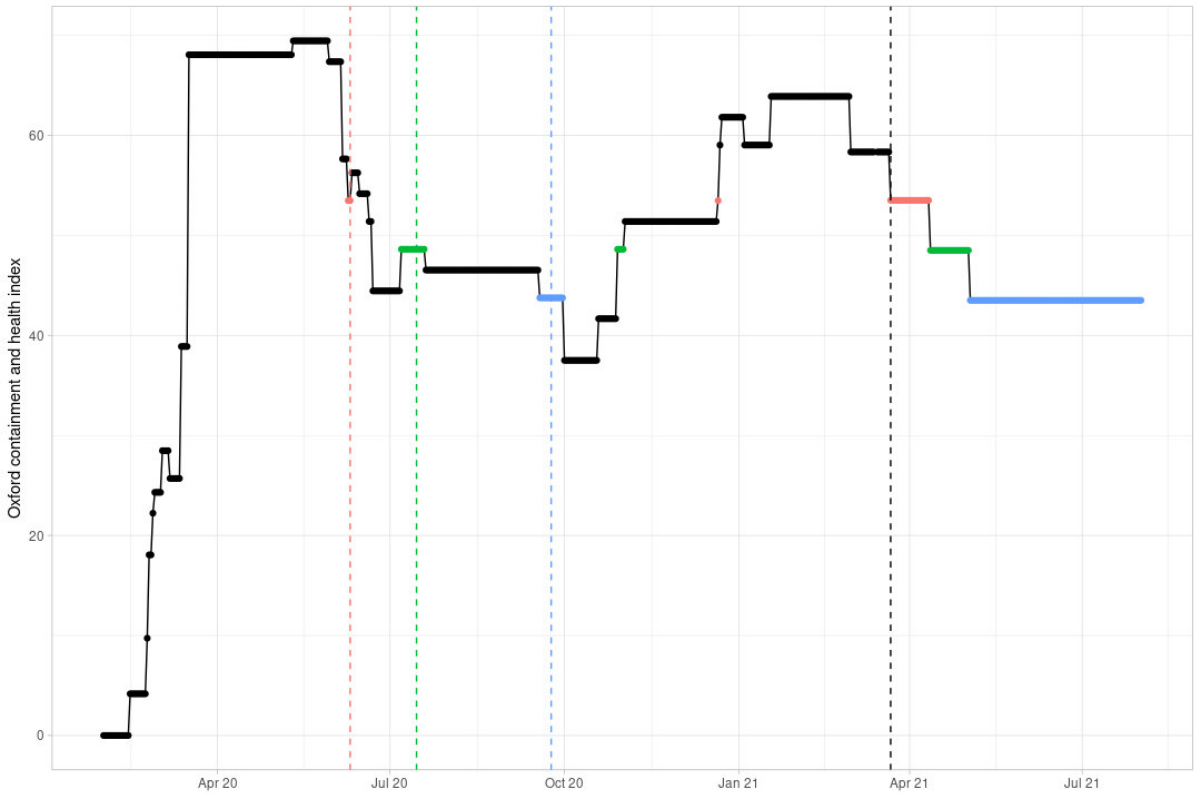

Figure S.7: Non-pharmaceutical interventions (NPIs) as Oxford Containment and Health Index over time in Switzerland as implemented at the national level. The depicted NPI relaxation scenario corresponds to the red NPI relaxation scenario from manuscript Figure 2. The red scenario represents five NPI relaxation steps, from 58.5 to 53.5 on 22 March, to 48.5 on 12 April and to 43.5 on 5 May 2021. The vertical dashed black line represents 22 March 2021, the date of the first potential NPI release that was simulated. The colours of the future scenario and the coloured vertical lines highlight the dates when previous NPIs were at a similar level to the future opening steps. Higher values depict stricter measures.

Prognosis probabilities

Once infected with SARS-CoV-2 and following a latent period, an infected individual develops either asymptomatic, mild, or severe disease. Individuals that develop severe disease may, after some time, either seek hospital care or remain outside of the hospital setting (e.g., within care homes). We model three distinct prognosis tracks for those that will seek hospital care: 1) the patient will eventually recover without intensive care, 2) the patient will require intensive care but will eventually recover, and 3) the patient will require intensive care and will ultimately die from COVID-19-related complications. See manuscript Figure 1 for an illustration of modelled natural history and prognosis pathways. We quantified age-group stratified probabilities for each prognosis (Table S.4) using age-disaggregated morbidity and mortality data from international sources (51, 52), Swiss-specific sources (1, 53), and a Swiss COVID-19 hospitalisation database (not publicly available). Once infected, a prognosis is derived for all individuals by stochastically sampling from a uniform distribution.

The prognosis probabilities given in Table S.4 assume an equal probability of infection across all age groups. Whilst the probability of infection in any given contact is not assumed to be age-

dependent (see *Infectiousness per contact* section), the number of contacts for any given person is age-dependent (see Figure S.4 in *Contact network* section). Therefore, each age-dependent prognosis probability needs to be scaled by an age-correction factor to convert to per-infection probabilities. Three additional factors can affect these age-related prognosis probabilities:

1. Improved care procedures (see improved_care_factor, Table S.1)
2. Increased mortality of viral variant infected with (Table S.2)
3. Symptom reducing effect of vaccination

The *improved care* factor represents the reduction in hospitalized COVID-19 cases requiring intensive care due to improved triage, use of treatments such as dexamethasone, and other factors. This improved care factor is calibrated, and assumed to take an effect on 1st June 2020 following the 'first wave' experienced in Switzerland. For individuals infected following vaccination, an age-dependent prognosis is initially derived as described above. A further probability of being asymptomatic instead of symptomatic is then calculated by multiplying the *symptom reducing effect* of the vaccine with the normalized level of vaccine efficacy at that point in time (see *Vaccine properties* section).

Table S.4: Age-group dependent probabilities of a given prognosis (52)

Age group	Asymptomatic	Mild disease	Severe disease	Critical disease	Death
0-10	30%	69.93%	0.07%	0.00%	<0.0001%
10-20	30%	69.79%	0.20%	0.01%	<0.0001%
20-30	30%	69.16%	0.80%	0.04%	<0.0001%
30-40	30%	67.76%	2.13%	0.11%	0.0002%
40-50	30%	66.57%	3.21%	0.21%	0.0014%
50-60	30%	62.86%	6.27%	0.85%	0.0193%
60-70	30%	58.38%	8.44%	2.95%	0.23%
70-80	30%	52.99%	9.66%	5.56%	1.79%
80-90+	30%	50.89%	5.56%	1.63%	11.92%

Infection, disease, and hospitalisation durations

Upon infection, the duration for which an individual will remain in each disease or care state is sampled from a distribution, as illustrated in Figure S.8, and described in Table S.1 (including sources for the best estimated values for each duration).

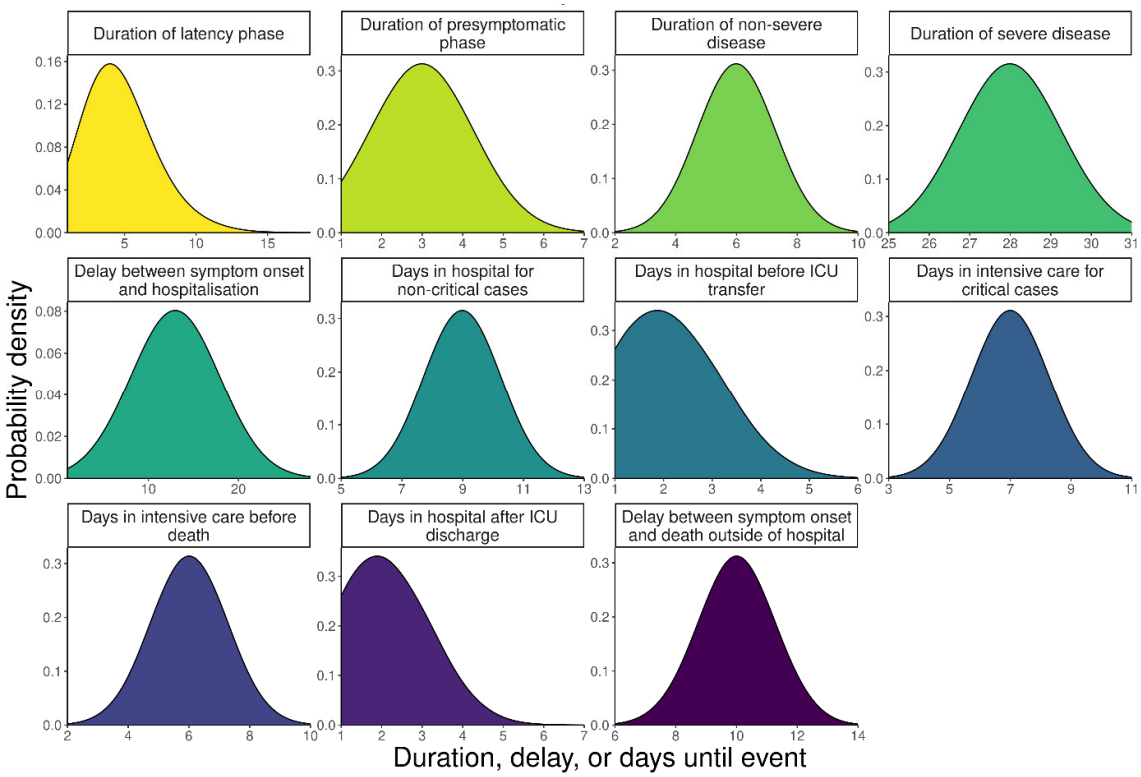

Figure S.8: Distributions of disease- and care-related durations used in this OpenCOVID application for Switzerland

Testing, diagnosis, and isolation

Upon infection, an individual is assigned a date at which they may potentially seek a test and be diagnosed as a confirmed COVID-19 case. The delay between symptom onset and a potential diagnosis for each individual is sampled from a truncated Gaussian distribution (Figure S.8). We derive the number of diagnoses over time directly from observed data of confirmed COVID-19 cases (Figure S.1) and apply the relevant number of diagnoses per day across the modelled population. By definition, all COVID-19 cases that seek hospital care receive a diagnosis. After taking hospitalised diagnoses into account, other individuals with severe disease outside of the hospital setting and individuals with mild disease are randomly selected as those who seek testing and are assigned a diagnosis in the model. To represent future test-seeking behaviour, the model-calculated proportion of cases diagnosed per infected case over the past 14-days is fixed into the future (Figure S.9). We note here that this assumption is not robust to major changes in testing policies or behaviours, including, but not limited to, mass testing. We assume no change in behaviour for individuals who test negative, and further assume that all non-severe cases isolate for a 10-day period immediately following diagnosis.

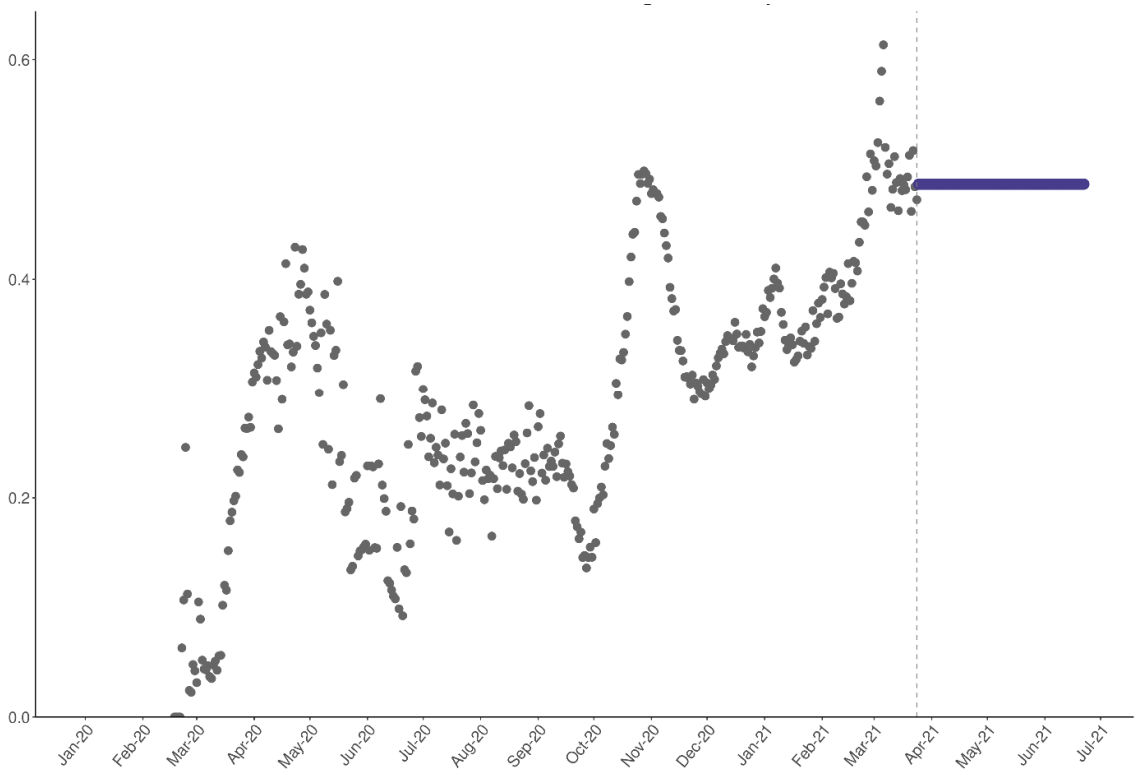

Figure S.9: Proportion of projected new COVID-19 diagnoses per infected case over time in Switzerland. Blue points (connected into a line) represent the assumed testing and diagnosis during the simulation period (from the end of March).

Immunity

For individuals that recover from SARS-CoV-2, we assume a partial acquired immunity of 83% to future infection upon recovery regardless of disease severity, risk group, or age (54-56). For the relatively short-term projections presented in this application to Switzerland, we assumed no waning of acquired immunity (Figure S.10). We note here that this optimistic assumption may not be appropriate for longer-term projections. In future work, the assumptions regarding level of immunity by disease state and waning acquired immunity will likely be reassessed as new evidence becomes available.

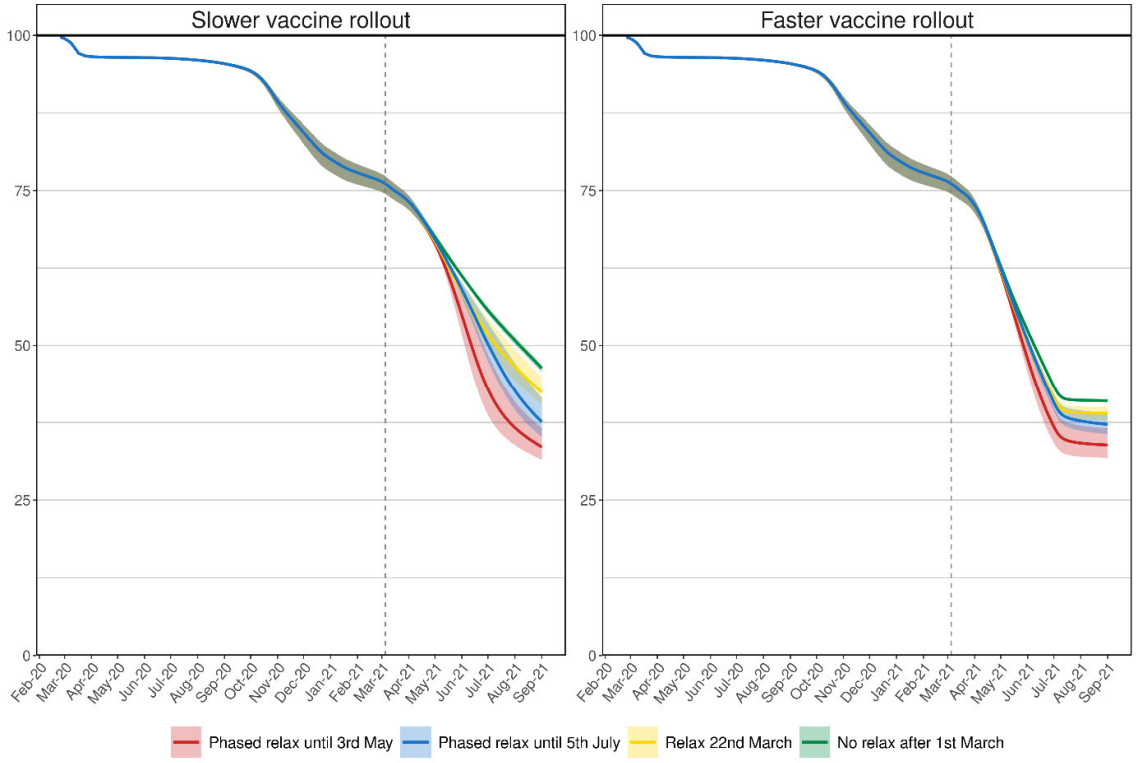

Figure S.10: Development of population susceptibility levels of scenarios 1A-1D over time. Population susceptibility is the complement of population immunity. The colours are the scenarios from manuscript Figure 2.

Vaccine properties

Vaccine efficacy following two doses was assumed to depend on vaccine type. For the mRNA vaccines (Pfizer and Moderna), an efficacy of 95% was assumed for all priority groups P1–P5. We implemented the vaccination of an individual as the smooth increase in immunity over time using a sigmoidal function that has a lower asymptote of 0, an upper asymptote of overall 'vaccine efficacy' (95% for Pfizer and Moderna, 62% for AstraZeneca) and an inflection point 14-days after vaccination. The growth rate of this curve is such that vaccine efficacy is close to zero on the day of vaccination, and is closer to full 'vaccine efficacy' after 28-days (Figure S.11).

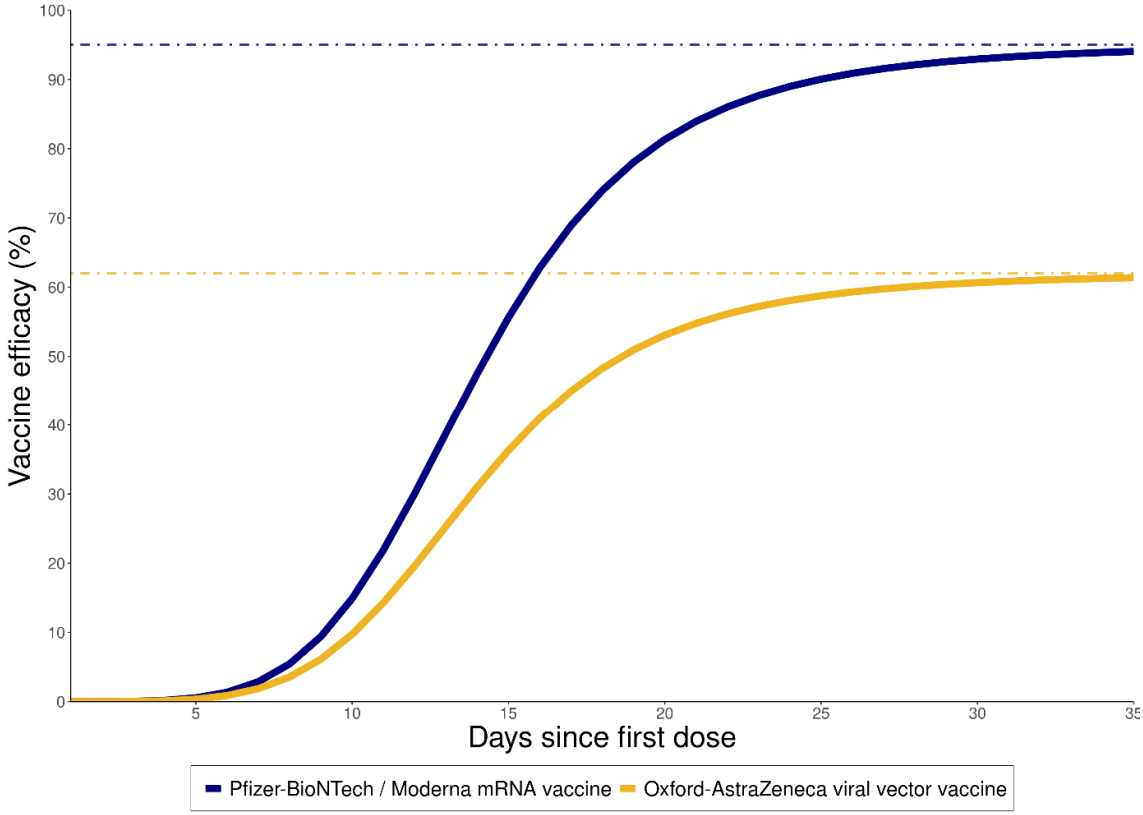

Figure S.11: Development of vaccine efficacy from day of receiving a first dose. Shown in blue is the development of immunity for a two-dose course with an mRNA vaccine, and in yellow for a two-dose course of the AstraZeneca viral vector vaccine. The vaccine efficacy is the combined effect of immunity and the reduction of severe disease. It is assumed that the second dose is given according to schedule within 28 days depending on vaccine, but not modelled explicitly.

Most vaccine trials claim to reduce COVID-19 symptom development as well as disease severity, however it remains unclear to what extent they prevent transmission. As a baseline, we assume mRNA vaccines are 80% effective in preventing infection (and future transmission) when at full efficacy. We then calculate the additional effectiveness of the vaccine to reduce symptoms such that the total reduction in symptoms among those vaccinated when the vaccine is at full efficacy (that is, 95% from 28 days after receiving the first dose).

By definition we have that:

$$\theta = 1 - (1 - \alpha) \cdot (1 - \gamma)$$

Where θ is the overall efficacy of the vaccine in symptomatic COVID-19, α is the transmission blocking effect, and γ is the additional symptom reducing effect. Solving for γ, we have:

$$\gamma = 1 - \frac{(1 - \theta)}{(1 - \alpha)}$$

In this application, we assess the sensitivity of model outputs to different assumptions of the vaccine fully protecting from infection (sterile immunity and preventing onward transmission). Namely, values of 60% and 95% for sterile immunity. The corresponding additional symptom reducing effect in each case is reported in Table S.5.

Table S.5: Vaccine properties under different assumptions of vaccine transmission blocking effect

Vaccine type	Overall efficacy (θ)	Sterile immunity effect (α)	Symptom reducing effect (γ)
mRNA	95%	80%	75%
mRNA	95%	60%	87.5%
mRNA	95%	95%	0%

Vaccine rollout

Vaccination strategies were modelled according to FOPH priority groups and updated (10 February 2021) after input from FOPH and other experts to reflect current rollout realisation (Table S.6). We assumed a baseline coverage of 75% across all priority groups for most scenarios. For scenarios 4A) and 4B) we modelled 60% and 90% coverage for priority groups P2 – P5 as a sensitivity analysis. We assumed either 50,000 or 100,000 vaccine doses used per day from 1 April 2021, which is within the bounds of the maximum vaccine availability as expected by the FOPH. Until 5 March we use data for number of doses used as provided by FOPH and scale linearly from there up to the target daily doses by 1 April. With 100,000 doses per day the target coverage of 75% across all groups will be reached before July 2021, with 50,000 doses per day it will not be reached before the end of the simulation in September 2021. OpenCOVID vaccinates people strictly according to priority groups, with the highest priority group receiving all doses until the target coverage is reached. Vaccines from CureVac, Novavax, and AstraZeneca were not incorporated in our projections.

Table S.6: Vaccine priority groups based on FOPH priority groups and modified after discussion with FOPH

Priority group	Description	Number of model-eligible people
P1	Aged over 75 years	756,400
P2	Aged between 65 and 75 years, under 65 with comorbidities, and healthcare workers	2,031,600 (850,000, 621,600, and 560,000, respectively)
P3	Household members of high-risk people	1,243,000
P4	Adults (18-64 years) in communal facilities and their caregivers	100,000
P5	All other adults (18-65 years)	4,414,600

Simulation details

Model simulations were initiated on 18th February 2020, 7-days before the first cases were confirmed for three consecutive days in Switzerland (25 to 28 February 2020). All model processes were computed at time intervals representing one day. One million individuals were modelled for simulations reported here, with a population scaling factor subsequently applied to all relevant model outputs to represent a one-to-one scale for the Swiss population. Where appropriate, metrics were disaggregated by age, variant of infection, and vaccine priority group. All model simulations were performed at sciCORE (37) maintained by the Scientific Computing Center at University of Basel.

Retrospective validation

A retrospective analysis was conducted at the end of October 2021 to examine how the actual observed data compared with our scenario design and model outcomes. We first compared our scenario design to the actual number of COVID-19 vaccine doses administered per day and the Oxford Containment and Heath Index (OCHI) associated with the actual NPI implementation. We then compared outcomes from the most comparable model scenario with observed confirmed cases, cases that were in hospital, cases that were in ICU, and COVID-19-related deaths reported between 6 March and 1 September 2021 in Switzerland (57).

Switzerland had planned for a rapid scale-up of vaccinations of up to 100,000 doses administered per day from early March 2021 (1). This level was eventually achieved, however scale-up ended up being somewhat slower than originally planned (Figure S.12b). Since we designed our vaccine scenarios on anticipated rollout and uptake, neither the ambitious (100,000 doses per day) nor conservative (50,000 doses per day) scenario truly reflect the actual vaccination campaign due to this delay in scale-up. Moreover, whilst none of our modelled scenarios exactly reflect the NPI and vaccine rollout strategies as they actually occurred in Switzerland from March to September 2021, we believe the scenario that most closely represents the actual implementation is Scenario 1C; relax 22 March with fast vaccine rollout (yellow curves, manuscript Figure 2 and Figure S.12). In general, the magnitude of the peaks in this scenario are approximately represented by the data for each metric, however, the timing is not well captured – as peaks were observed quicker than the model had predicted ((c), (d), and (e) of Figure S.12). Numerous factors could be contributing to this, including 1) the vaccine scale-up being slower than anticipated, 2) changing attitudes around NPI adherence following the second wave and as vaccines where being rolled out in Switzerland, 3) the OCHI not accurately capturing future changes of NPI intensity, and 4) infectiousness of VOCs. At the time of analysis, less was known about the infectiousness of the B.1.1.7 variant, which was potentially higher than what was modelled (refer to the sensitivity analysis as shown in Figure 6 with details described in Table 2 from the manuscript).

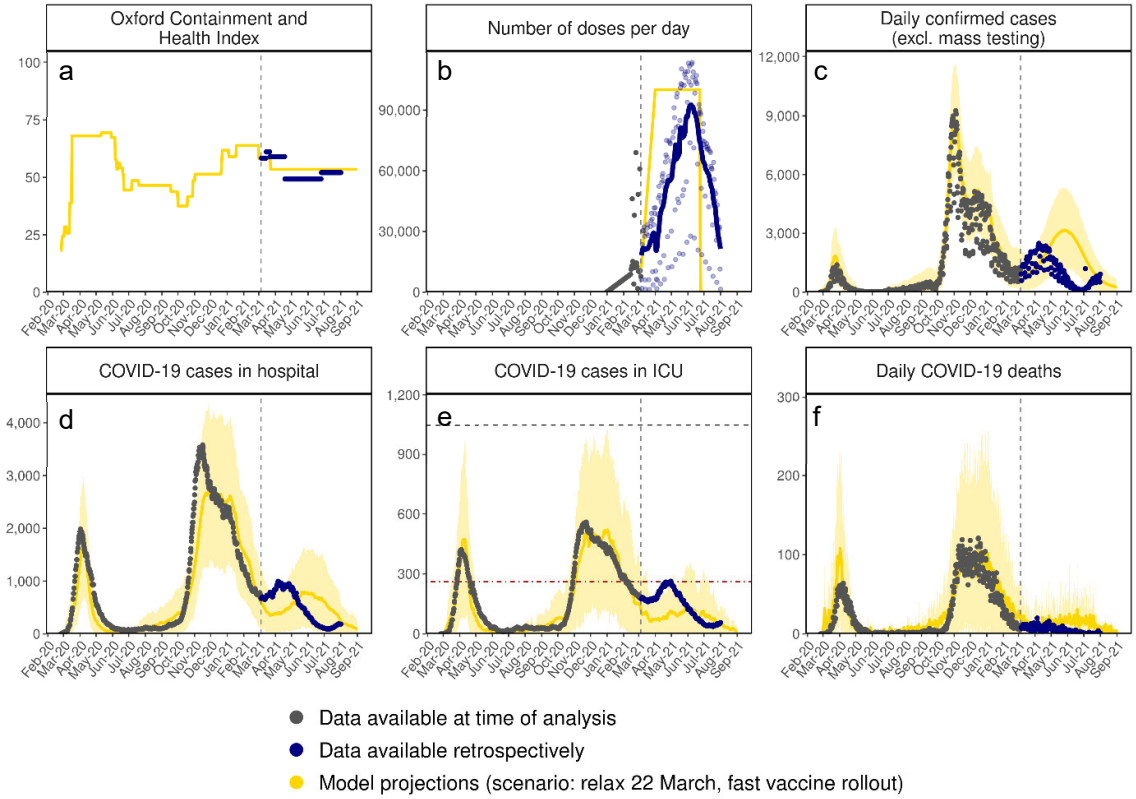

Figure S.12: Retrospective comparison of actual data with Scenarios 1C. (a) Oxford Containment and Health Index (OCHI) values, (b) COVID-19 vaccine doses administered per day with a seven-day rolling average, (c) daily COVID-19 confirmed cases, (d) new daily COVID-19 hospital admissions, (e) new daily ICU admissions, and (f) daily COVID-19 deaths. Modelled scenario 1C (relax 22 March 2021, fast vaccine rollout) is represented by the yellow curves, data available at the time of analysis are in grey, and data available retrospectively are in blue.

In general, the model was too optimistic in terms of ICU occupancy, and too pessimistic in terms of deaths (Figure S.12 (e) and (f)). Historically, the model accurately captured the relationship between ICU occupancy and mortality; however, as vaccines were being rolled out, the model was not able to reflect some of the observed de-coupling for several reasons related to vaccine coverage and care seeking patterns. Foremost, Switzerland achieved a higher vaccine coverage among those most at risk of COVID-19-related death (70-79 and 80 years and older) than the assumed 75% coverage (Figure S.13). This has likely contributed to the overestimate of deaths. Furthermore, vaccine coverage below the 75% coverage level assumed among age groups 30-39, 40-49, and 50-59 was actually observed. Individuals in these age groups are more likely to require hospital and ICU care relative to their risk of death, which may be contributing to the underestimate of ICU occupancy. Figure S.13 shows a comparison of vaccine coverage by age group assumed for the faster vaccine rollout scenario (100,000 doses per day) in the model with the actual rollout. It was assumed that priority groups (P1-P5, as described in Table 2 from the manuscript) would sequentially reach 75% vaccine coverage, considering acceptance rate.

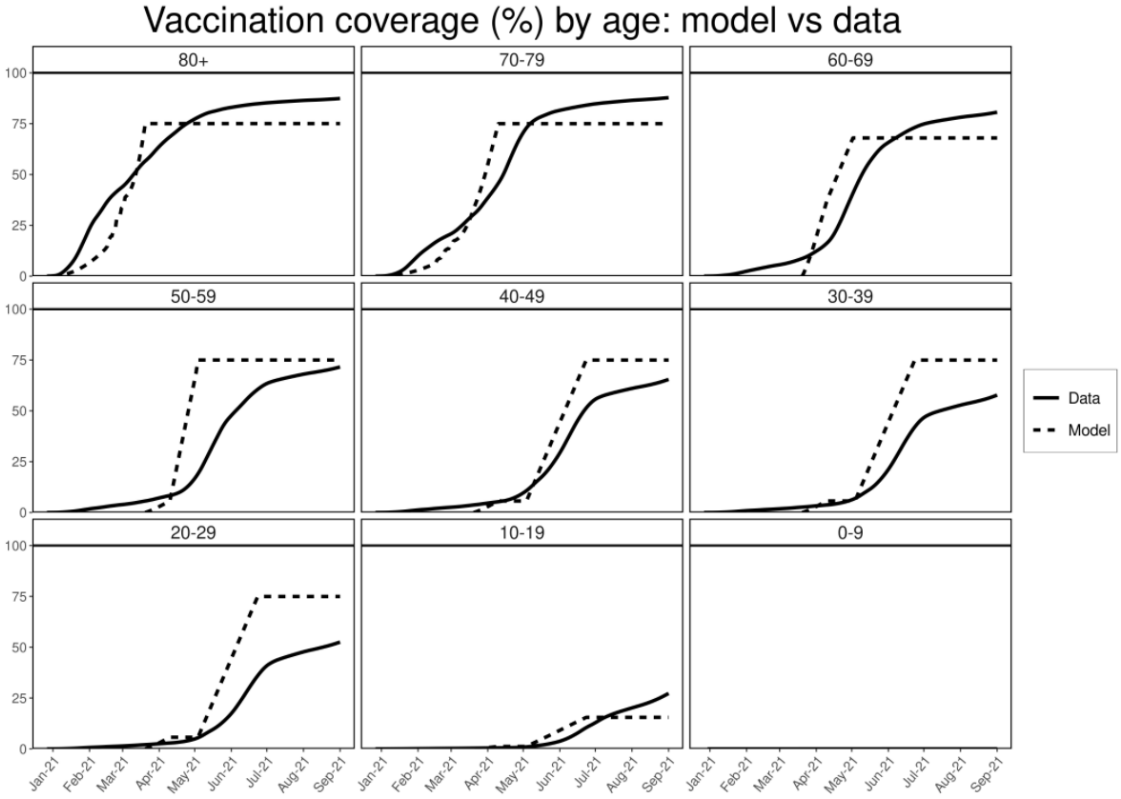

Figure S.13: Data versus model assumptions for the faster vaccine rollout (100,000 doses per day) by age group in Switzerland. Dashed curves represent vaccine coverage for each age group assumed during the simulation from 6 March to 1 September 2021 with vaccination modelled in those 18 years and older. Solid curves represent actually observed vaccine coverage in Switzerland from the start of rollout until the end of the simulation. At the time of this analysis, COVID-19 vaccines were not authorized for administration to children 17 years and younger.

Model development and maintenance

OpenCOVID is written primarily in the R programming language (58) and is stable with R version 3.6.0. The code for OpenCOVID is open source, and available from the Swiss TPH GitHub (59). Due to the level of computational power required to calibrate the model and simulate scenarios, the model pipeline makes use of a SLURM based cluster sciCORE (37) maintained by the Scientific Computing Center at the University of Basel. Interactions to the cluster are written in bash script. The authors of the manuscript maintain the model source code.

References

1. FOPH. Coronavirus: Situation in Switzerland, as of 22 March 2021 Liebefeld, Switzerland: Federal Office of Public Health; 2021 [Available from: https://www.bag.admin.ch/bag/de/home/krankheiten/ausbrueche-epidemien-pandemien/aktuelle-ausbrueche-epidemien/novel-cov/situation-schweiz-und-international.html].

2. Chen C, Nadeau SA, Topolsky I, Manceau M, Huisman JS, Jablonski KP, et al. Quantification of the spread of SARS-CoV-2 variant B.1.1.7 in Switzerland. Epidemics. 2021;37:100480. htpps://10.1016/j.epidem.2021.100480.

3. Byambasuren O, Cardona M, Bell K, Clark J, McLaws M-L, P G. Estimating the extent of true asymptomatic COVID-19 and its potential for community transmission: systematic review and meta-analysis. Journal of the Association of Medical Microbiology and Infectious Disease Canada. 2020;5(4):223-34. htpps://10.3138/jammi-2020-0030.

4. Gudbjartsson DF, Helgason A, Jonsson H, Magnusson OT, Melsted P, Norddahl GL, et al. Spread of SARS-CoV-2 in the Icelandic Population. N Engl J Med. 2020;382(24):2302-15. htpps://10.1056/NEJMoa2006100.

5. Mizumoto K, Kagaya K, Zarebski A, Chowell G. Estimating the asymptomatic proportion of coronavirus disease 2019 (COVID-19) cases on board the Diamond Princess cruise ship, Yokohama, Japan, 2020. Euro Surveill. 2020;25(10) htpps://10.2807/1560-7917.Es.2020.25.10.2000180.

6. Nishiura H, Kobayashi T, Miyama T, Suzuki A, Jung SM, Hayashi K, et al. Estimation of the asymptomatic ratio of novel coronavirus infections (COVID-19). Int J Infect Dis. 2020;94:154-5. htpps://10.1016/j.ijid.2020.03.020.

7. Qiu J. Covert coronavirus infections could be seeding new outbreaks. Nature News. 2020 20 March.

8. Wu J, Liu X, Zhou D, Qiu G, Dai M, Yang Q, et al. Identification of RT-PCR-Negative Asymptomatic COVID-19 Patients via Serological Testing. Front Public Health. 2020;8:267. htpps://10.3389/fpubh.2020.00267.

9. Kissler SM, Fauver JR, Mack C, Olesen SW, Tai C, Shiue KY, et al. Viral dynamics of acute SARS-CoV-2 infection and applications to diagnostic and public health strategies. PLoS Biol. 2021;19(7):e3001333. htpps://10.1371/journal.pbio.3001333.

10. Lauer SA, Grantz KH, Bi Q, Jones FK, Zheng Q, Meredith HR, et al. The Incubation Period of Coronavirus Disease 2019 (COVID-19) From Publicly Reported Confirmed Cases: Estimation and Application. Ann Intern Med. 2020;172(9):577-82. htpps://10.7326/m20-0504.

11. Lei S, Jiang F, Su W, Chen C, Chen J, Mei W, et al. Clinical characteristics and outcomes of patients undergoing surgeries during the incubation period of COVID-19 infection. EClinicalMedicine. 2020;21:100331. htpps://10.1016/j.eclinm.2020.100331.

12. Read JM, Bridgen JRE, Cummings DAT, Ho A, Jewell CP. Novel coronavirus 2019-nCoV (COVID-19): early estimation of epidemiological parameters and epidemic size

estimates. Philos Trans R Soc Lond B Biol Sci. 2021;376(1829):20200265. htpps://10.1098/rstb.2020.0265.

13. Zhao C, Xu Y, Zhang X, Zhong Y, Long L, Zhan W, et al. Public health initiatives from hospitalized patients with COVID-19, China. J Infect Public Health. 2020;13(9):1229-36. htpps://10.1016/j.jiph.2020.06.013.

14. Hale T, Angrist N, Goldszmidt R, Kira B, Petherick A, Phillips T, et al. A global panel database of pandemic policies (Oxford COVID-19 Government Response Tracker). Nature Human Behaviour. 2021;5(4):529-38. DOI: 10.1038/s41562-021-01079-8.

15. Du Z, Xu X, Wu Y, Wang L, Cowling BJ, Meyers LA. The serial interval of COVID-19 from publicly reported confirmed cases. medRxiv. 2020 htpps://10.1101/2020.02.19.20025452.

16. Wölfel R, Corman VM, Guggemos W, Seilmaier M, Zange S, Müller MA, et al. Virological assessment of hospitalized patients with COVID-2019. Nature. 2020;581(7809):465-9. htpps://10.1038/s41586-020-2196-x.

17. Hua J, Chen R, Zhao L, Wu X, Guo Q, He C, et al. Epidemiological features and medical care-seeking process of patients with COVID-19 in Wuhan, China. ERJ Open Research. 2020;6(2):00142-2020. htpps://10.1183/23120541.00142-2020.

18. Peirlinck M, Linka K, Sahli Costabal F, Kuhl E. Outbreak dynamics of COVID-19 in China and the United States. Biomech Model Mechanobiol. 2020;19(6):2179-93. htpps://10.1007/s10237-020-01332-5.

19. Phares TW, Kotraiah V, Karunarathne DS, Huang J, Browne CD, Buontempo P, et al. A Peptide-Based PD1 Antagonist Enhances T-Cell Priming and Efficacy of a Prophylactic Malaria Vaccine and Promotes Survival in a Lethal Malaria Model. Front Immunol. 2020;11:1377. htpps://10.3389/fimmu.2020.01377.

20. Zhao W, Zha X, Li T, Li A, Yu S. Clinical Characteristics and Durations of Hospitalized Patients with COVID-19 in Beijing: A Retrospective Cohort Study. Cardiovascular Innovations and Applications. 2021;6(1):33-44. htpps://10.15212/CVIA.2021.0019.

21. ECDC. Projected baselines of COVID-19 in the EU/EEA and the UK for assessing the impact of de-escalation of measures – 26 May 2020 Stockholm: European Centre for Disease Prevention and Control; 2020 [Available from: https://www.ecdc.europa.eu/sites/default/files/documents/Projected-baselines-COVID-19-for-assessing-impact-measures.pdf].

22. ECDC. The European Surveillance System (TESSy) Stockholm: European Centre for Disease Prevention and Control 2020 [Available from: https://www.ecdc.europa.eu/en/publications-data/european-surveillancesystem-tessy].

23. Linton NM, Kobayashi T, Yang Y, Hayashi K, Akhmetzhanov AR, Jung SM, et al. Incubation Period and Other Epidemiological Characteristics of 2019 Novel Coronavirus Infections with Right Truncation: A Statistical Analysis of Publicly Available Case Data. J Clin Med. 2020;9(2) htpps://10.3390/jcm9020538.

24. Kretzschmar ME, Rozhnova G, Bootsma MCJ, van Boven M, van de Wijgert J, Bonten MJM. Impact of delays on effectiveness of contact tracing strategies for COVID-19: a

modelling study. Lancet Public Health. 2020;5(8):e452-e9. htpps://10.1016/s2468-2667(20)30157-2.

25. Flaxman S, Mishra S, Gandy A, Unwin HJT, Mellan TA, Coupland H, et al. Estimating the effects of non-pharmaceutical interventions on COVID-19 in Europe. Nature. 2020;584(7820):257-61. htpps://10.1038/s41586-020-2405-7.

26. Thai PQ, Toan DTT, Son DT, Van HTH, Minh LN, Hung LX, et al. Factors associated with the duration of hospitalisation among COVID-19 patients in Vietnam: A survival analysis. Epidemiol Infect. 2020;148:e114. htpps://10.1017/s0950268820001259.

27. Horby P, Lim WS, Emberson JR, Mafham M, Bell JL, Linsell L, et al. Dexamethasone in Hospitalized Patients with Covid-19. N Engl J Med. 2021;384(8):693-704. htpps://10.1056/NEJMoa2021436.

28. Hall VJ, Foulkes S, Charlett A, Atti A, Monk EJM, Simmons R, et al. SARS-CoV-2 infection rates of antibody-positive compared with antibody-negative health-care workers in England: a large, multicentre, prospective cohort study (SIREN). Lancet. 2021;397(10283):1459-69. htpps://10.1016/s0140-6736(21)00675-9.

29. Mahase E. Covid-19: Past infection provides 83% protection for five months but may not stop transmission, study finds. BMJ. 2021;372:n124. htpps://10.1136/bmj.n124.

30. Hunter PR, Brainard J. Estimating the effectiveness of the Pfizer COVID-19 BNT162b2 vaccine after a single dose. A reanalysis of a study of 'real-world' vaccination outcomes from Israel. medRxiv. 2021:2021.02.01.21250957. htpps://10.1101/2021.02.01.21250957.

31. Groves DC, Rowland-Jones SL, Angyal A. The D614G mutations in the SARS-CoV-2 spike protein: Implications for viral infectivity, disease severity and vaccine design. Biochem Biophys Res Commun. 2021;538:104-7. htpps://10.1016/j.bbrc.2020.10.109.

32. Davies NG, Jarvis CI, van Zandvoort K, Clifford S, Sun FY, Funk S, et al. Increased mortality in community-tested cases of SARS-CoV-2 lineage B.1.1.7. Nature. 2021;593(7858):270-4. htpps://10.1038/s41586-021-03426-1.

33. Tzou PL, Tao K, Nouhin J, Rhee SY, Hu BD, Pai S, et al. Coronavirus Antiviral Research Database (CoV-RDB): An Online Database Designed to Facilitate Comparisons between Candidate Anti-Coronavirus Compounds. Viruses. 2020;12(9). htpps://10.3390/v12091006.

34. Davies NG, Abbott S, Barnard RC, Jarvis CI, Kucharski AJ, Munday JD, et al. Estimated transmissibility and impact of SARS-CoV-2 lineage B.1.1.7 in England. Science. 2021;372(6538). htpps://10.1126/science.abg3055.

35. Ramanathan M, Ferguson ID, Miao W, Khavari PA. SARS-CoV-2 B.1.1.7 and B.1.351 Spike variants bind human ACE2 with increased affinity. bioRxiv [Preprint]. 2021. htpps://10.1101/2021.02.22.432359.

36. Korber B, Fischer WM, Gnanakaran S, Yoon H, Theiler J, Abfalterer W, et al. Tracking Changes in SARS-CoV-2 Spike: Evidence that D614G Increases Infectivity of the COVID-19 Virus. Cell. 2020;182(4):812-27.e19. htpps://10.1016/j.cell.2020.06.043.

37. UniBasel. sciCORE scientific computing core facility Basel, Switzerland: University of Basel; 2021 [Available from: https://scicore.unibas.ch/].

38. Binois M, Gramacy R. hetGP: Heteroskedastic Gaussian process modeling and sequential design in R 2019 [Available from: https://cranr-projectorg/web/packages/hetGP/vignettes/hetGP_vignettepdf].

39. Binois M, Gramacy RB, Ludkovski M. Practical Heteroscedastic Gaussian Process Modeling for Large Simulation Experiments. Journal of Computational and Graphical Statistics. 2018;27(4):808-21. htpps://10.1080/10618600.2018.1458625.

40. Mossong J, Hens N, Jit M, Beutels P, Auranen K, Mikolajczyk R, et al. Social contacts and mixing patterns relevant to the spread of infectious diseases. PLoS Med. 2008;5(3):e74. htpps://10.1371/journal.pmed.0050074.

41. Funk S. Socialmixr: Social Mixing Matrices for Infectious Disease Modelling. The Comprehensive R Archive Network 2018 [Available from: https://CRAN.R-project.org/package=socialmixr https://github.com/sbfnk/socialmixr].

42. Gebhard C, Regitz-Zagrosek V, Neuhauser HK, Morgan R, Klein SL. Impact of sex and gender on COVID-19 outcomes in Europe. Biol Sex Differ. 2020;11(1):29. htpps://10.1186/s13293-020-00304-9.

43. Jones TC, Biele G, Mühlemann B, Veith T, Schneider J, Beheim-Schwarzbach J, et al. Estimating infectiousness throughout SARS-CoV-2 infection course. Science. 2021;373(6551) DOI: 10.1126/science.abi5273.

44. Ferretti L, Ledda A, Wymant C, Zhao L, Ledda V, Abeler-Dörner L, et al. The timing of COVID-19 transmission. medRxiv. 2020:2020.09.04.20188516. htpps://10.1101/2020.09.04.20188516.

45. FSO. MeteoSwiss Neuchâtel: Federal Statistical Office; 2021 [Available from: https://www.meteoswiss.admin.ch/home.html?tab=overview].

46. FSO. Swiss public administration's central portal for open government data Neuchâtel: Federal Statistical Office; 2021 [Available from: https://opendata.swiss/en].

47. FSO. Climatological Network - Daily Values Neuchâtel: Federal Statistical Office; 2021 [Available from: https://opendata.swiss/en/dataset/klimamessnetz-tageswerte].

48. Cordano E, E. E. Package 'RMAWGEN': Multi-Site Auto-Regressive Weather GENerator 2019 [Available from: https://cran.r-project.org/web/packages/RMAWGEN/RMAWGEN.pdf].

49. SwissTPH. COVID measures by canton Basel, Switzerland: Swiss Tropical and Public Health Institute; 2021 [Available from: https://github.com/SwissTPH/COVID_measures_by_canton].

50. FOPH. COVID-19 Switzerland: Further procedures with regard to the national measures, dated 17 February 2021 Liebefeld, Switzerland: Federal Office of Public Health; 2021 [Available from: https://www.bag.admin.ch/dam/bag/de/dokumente/mt/k-und-i/aktuelle-ausbrueche-pandemien/2019-nCoV/Unterlagen-Konsultationen-

Kantone/begleitdokument-bes-lage-lockerung-1.pdf.download.pdf/Begleitdokument%20f%C3%BCr%20die%20Kantone.pdf].

51. Verity R, Okell LC, Dorigatti I, Winskill P, Whittaker C, Imai N, et al. Estimates of the severity of coronavirus disease 2019: a model-based analysis. Lancet Infect Dis. 2020;20(6):669-77. htpps://10.1016/s1473-3099(20)30243-7.

52. Ferguson NM, Laydon D, Nedjati-Gilani G, Imai N, Ainslie K, Baguelin M, et al. Report 9: Impact of non-pharmaceutical interventions (NPIs) to reduce COVID-19 mortality and healthcare demand. 2020 [Available from: https://www.imperial.ac.uk/media/imperial-college/medicine/sph/ide/gida-fellowships/Imperial-College-COVID19-NPI-modelling-16-03-2020.pdf].

53. Vaughan T, Chen C, Ashcroft P, Lethinen S, Angst D, S B, et al. CH Covid-19 Dashboard. Zurich, Switzerland: Swiss Federal Office of Public Health (FOPH) and OpenZH; 2021 [Available from: https://ibz-shiny.ethz.ch/covidDashboard/].

54. Edridge AWD, Kaczorowska J, Hoste ACR, Bakker M, Klein M, Loens K, et al. Seasonal coronavirus protective immunity is short-lasting. Nature Medicine. 2020;26(11):1691-3. htpps://10.1038/s41591-020-1083-1.

55. Good MF, Hawkes MT. The Interaction of Natural and Vaccine-Induced Immunity with Social Distancing Predicts the Evolution of the COVID-19 Pandemic. mBio. 2020;11(5) htpps://10.1128/mBio.02617-20.

56. Spellberg B, Nielsen TB, Casadevall A. Antibodies, Immunity, and COVID-19. JAMA Internal Medicine. 2021;181(4):460-2. htpps://10.1001/jamainternmed.2020.7986.

57. FOPH. Coronavirus: Situation in Switzerland, as of 28 October 2021 Liebefeld, Switzerland: Federal Office of Public Health; 2021 [Available from: https://www.bag.admin.ch/bag/de/home/krankheiten/ausbrueche-epidemien-pandemien/aktuelle-ausbrueche-epidemien/novel-cov/situation-schweiz-und-international.html].

58. Ihaka R, Gentleman R. R: A Language for Data Analysis and Graphics. Journal of Computational and Graphical Statistics. 1996;5(3):299-314. htpps://10.2307/1390807.

59. SwissTPH. OpenCOVID source code Basel, Switzerland: Swiss Tropical and Public Health Institute; 2021 [Available from: https://github.com/SwissTPH/OpenCOVID].